HOURGLASSIN'

RUBE AND SETH

Abstract. Abstract goes here

1. Introduction

We be MIG'n and hourglassin'.

2. Least-Squares Multi-Image Geopositioning With Many Images

2.1. **MIG.** Use least-squares to show $\lim_{n\to\inf} err = 0$.

2.2. **Simulation with Synthetic Imagery.** In this section we develop a large simulated testbed, and evaluate Least-squares MIG with various experimental measures for estimated error, on samples of randomly-selected subsets of images, of size ranging from 4 to 1000.

To develop the test set, we start with a large as possible set of real, unadjusted sensor models which have common overlap. From [1] we have 10 Worldview-1 sensor models which all view the ground location 36N 117.5W 1700mHAE (WGS84). This point is set as Ground Truth.

We then extend the set of real sensor models by random perturbation. We repeatedly add random amounts of correction to position and orientation adjustable parameters. The random corrections are sampled from uniform distributions with bounds many times the nominal triangulation defaults, with the aim of spreading the simulated sensors as uniformly as possible, minimizing clustering around the original sensor models. (See resulting clustering in Fig **??**). Most large random perturbations of this kind will steer the real sensor models away from viewing our truth point. Sensor models that still contain the truth point within their image bounds are retained, until we have 99 perturbations for each original, real sensor model, for a total of 1000 sensor models.

The simulated set of 1000 images thus constructed is considered the Truth set of sensor models, with position and orientation parameters that perfectly represent conditions at image collection, to which actual sensor models would be imperfect estimates. The sensor model's ground to image function is used to project the truth point into image coordinates for each sensor model. These image measurements are retained as truth as well. The ray bundle emanating from these truth image points intersect perfectly (to within computational precision of the image to ground function) at the truth point in ground space. Thus MIG would yield the truth ground point, for 1000 images or for any subset. Call this idealized set of images $\mathcal{I}$.

Once $\mathcal{I}$ is assembled, experiments can be conducted by adding a controlled amount of error (randomly sampled from a known distribution) to each sensor model. The 1000 sensor models thus perturbed represent a possible realization of

1000 images with position and orientation parameters being different from their actual truth. The idealized image measurements can be used (because that is where the visualization of the ground feature actually appears), a controlled amount of error can be added in image space (to represent a desired amount of image measurement error, or unmodeled sensor error). Using perturbed image measurements/sensor models, the resulting ray bundle will represent a realistic spread of image rays around the truth point, to which MIG and Hourglassing algorithms can be applied and evaluated. This procedure can be carried out for any subset of N images, in fact for any number of N-image samples.

Let $\mathcal{P}$ be the set of 1000 perturbed images. In this experiment, for each $N \in 4, 5, ...100, 105, 110, ...995, 1000$, subsets of N images are sampled from the $\mathcal{P}$ perturbed images $k = 100$ times (except for $N = 1000$, where the entire set is used only $k = 1$ times). MIG is used to estimate the geolocation of the point using the N-image subset. Because we know the truth ground point, the trivial intersection of $\mathcal{I}$, we can compute the actual error of each of these MIGs.

Figure 1 shows the reference variances of every MIG from this experiment. Reference variance is tightly clustered around 1, which demonstrates that the use of apriori covariance in the MIG calculations is consistent with the errors involved in the perturbation of $\mathcal{P}$.

Figure 2 shows the average of errors in the X, Y, and Z dimensions. Each point represents an average over $k = 100$ MIGS. Because errors in positive and negative directions cancel each other out in these averages, this graph shows the amount of bias in the MIG calculations across N-subsets. For the full set $\mathcal{P}$ ($N = 1000$), $dX \approx 0$, $dY \approx -3$cm, and $dZ \approx 5$cm. This is the overall error that perturbation introduced into $\mathcal{P}$, and it is clear that the average MIG converges to this, showing that the MIG is not a biased estimate.

To avoid positive and negative errors cancelling each other out, we switch to positive quantities. Figure 3 shows the average horizontal, vertical, and 3D error for each N. Each point represents $k = 100$ MIGs. To clarify the rate of convergence and separation of the curves, a logarithmic scale is used. Not surprisingly, vertical error is larger than horizontal.

Every MIG yields output covariance, the estimate of the accuracy of the MIG's geolocation result. Figure 4 shows (in log-scale) the average length of the large (generally vertical) and two smaller (generally horizontal) radii of the 1-sigma error ellipsoid. (TBD: change to CE90/LE90?) Figure 5 multiplies each point from Figure 4 by a factor of $\sqrt{N}$. The flatness of these curves demonstrates the thesis of this paper, that MIG follows the Law of Large Numbers, and exhibits error that decreases as $1/\sqrt{N}$. Figure 6 shows the actual average horizontal and vertical errors for each N, plotted against the error ellipsoid radii. Both are multiplied by $\sqrt{N}$, and the measured errors also have a finite population correction applied [3].

3. Hourglassin'

3.1. **Motivation.** Because available sensor models (such as RPC) often lack a meaningful error model to input to MIG, and for computational simplicity, we introduce a heuristic approach as an alternative to rigorous least-squares MIG. Although when visualized 'up close' to the true answer, any particular tangle of rays may seem unclear about where the ground point should be localized, from a global perspective, the ray bundle will be something like a cone, widening to the

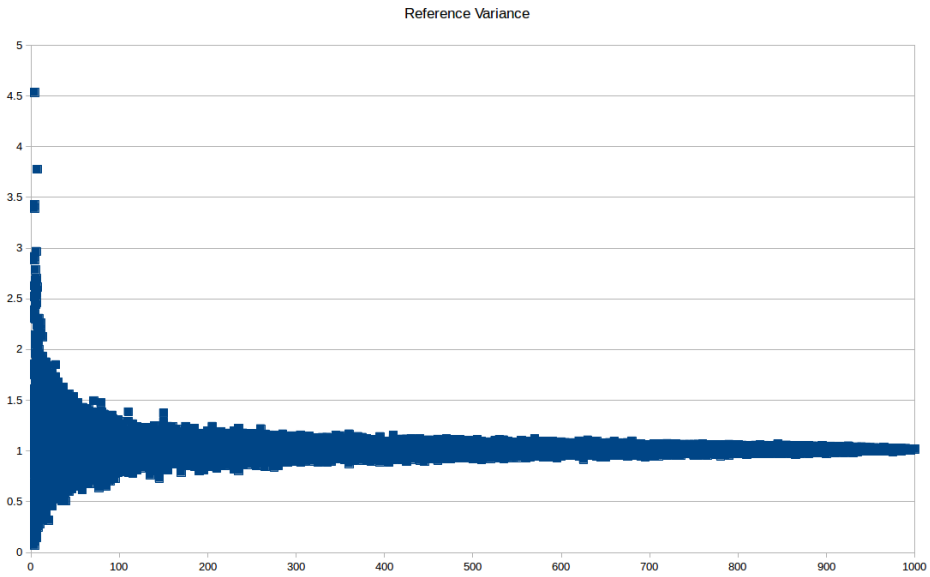

FIGURE 1. All reference variances

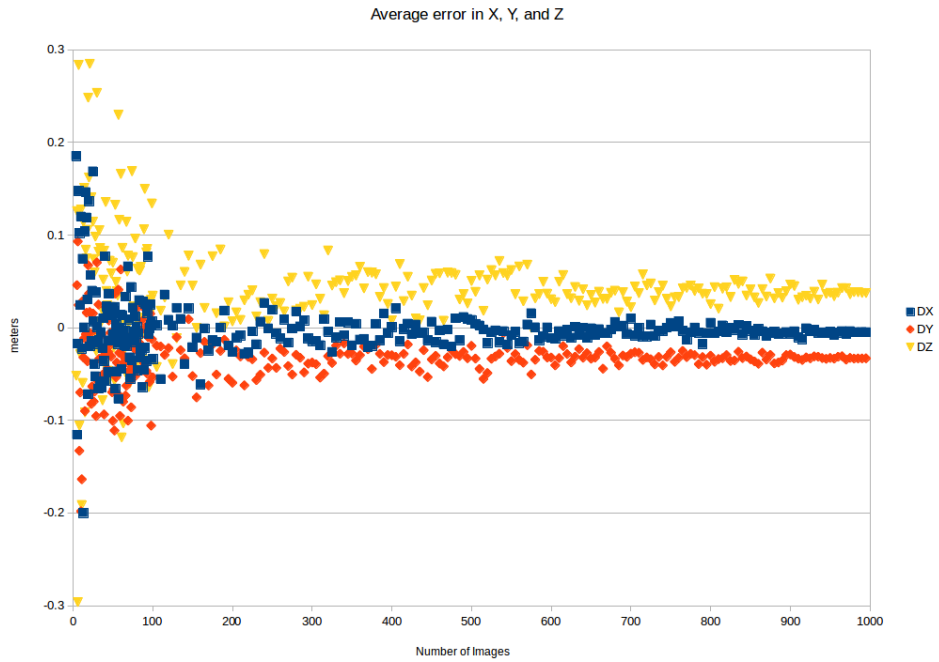

FIGURE 2. Average Errors in X, Y, and Z

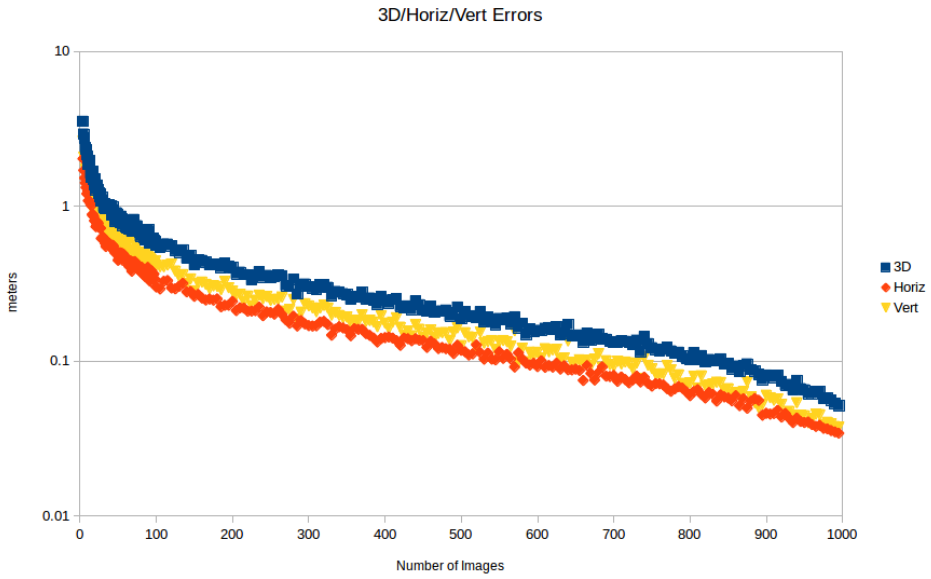

FIGURE 3. Average Horizontal, Vertical and 3D Errors (log scale)

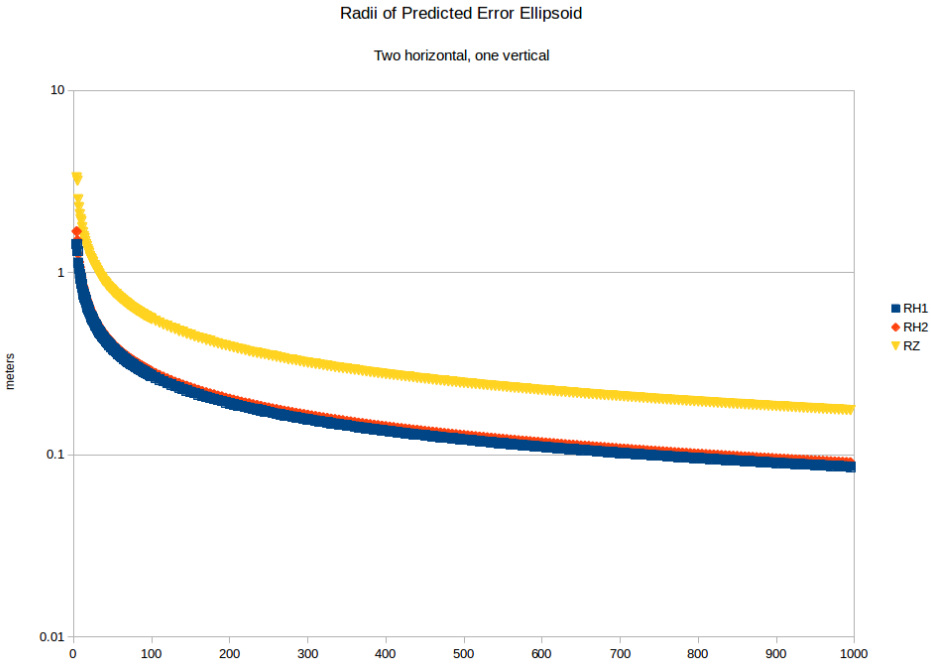

FIGURE 4. Average Radii of 1-sigma Error Ellipsoids (log scale)

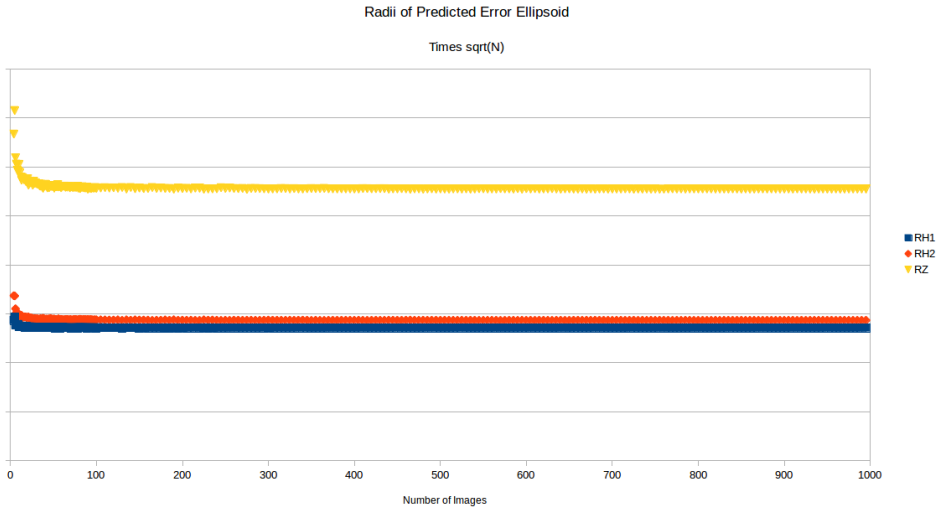

FIGURE 5. Average Ellipsoid Radii, multiplied by $\sqrt{N}$

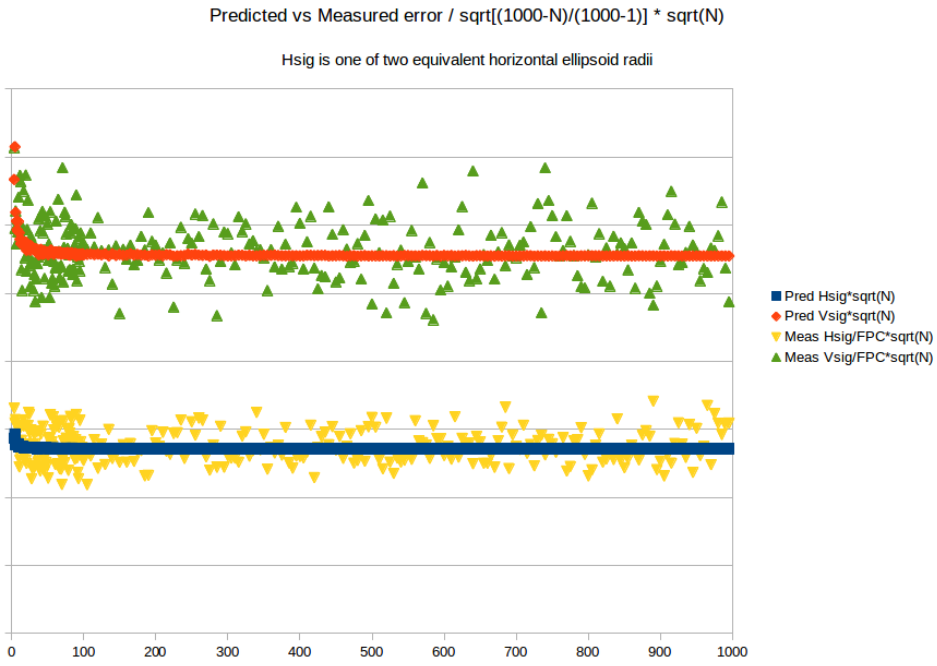

FIGURE 6. Predicted and Measured Errors

cluster of satellite (or airborne) perspective centers, narrowing at the ground point, and widening again beyond the ground point. We seek the answer at the narrowest point of the cone. In an ideal case, the ray bundle will intersect at a single point,

which has cross-sectional area of 0. In a real-world case, the bundle will appear as a cone with a 'fat' intersection. Thus the name 'hourglassing' to motivate the heuristic technique.

Given a bundle of rays, we can intersect the bundle with planes of various heights, compute the collection of intersections of the ray bundle with each height plane, measure the spread of the 2-D distribution of points, and choose the plane with the least spread to be the solution for the height of the desired ground point. For the horizontal location of the ground point, the natural choice is the mean of the intersection points in the chosen plane.

Rather than attacking this problem with a brute force search for the spread-minimizing by computing intersection sets at very many heights, and slicing height space sufficiently thin to achieve a desired vertical resolution, we attempt some theoretical underpinnings for this technique that will allow a more efficient and precise solution, and help motivate a meaningful estimate of the error of the resulting ground point.

3.2. **Computing height of minimum spread.** Assume two heights $z_+ > z_-$, and assume a set of N 3D lines L_i, none of which is horizontal. Specify the lines by their intersections with the planes of heights $z_\pm$ at points (x^i_+, y^i_+, z_+) and (x^i_-, y^i_-, z_-), for $i = 1 \dots N$.

Define

$$x^i(\lambda) = \lambda x^i_+ + (1-\lambda)x^i_-$$
$$y^i(\lambda) = \lambda y^i_+ + (1-\lambda)y^i_-$$
$$z(\lambda) = \lambda z_- + (1-\lambda)z_-$$

For any λ, $(x^i(\lambda), y^i(\lambda), z(\lambda))$ is a point on line L_i; whether $0 \le \lambda \le 1$ determines whether the point is an interpolation between or extrapolation beyond the $z_\pm$ planes (in either case, we will just use the term interpolated). Together, all the points $(x^i(\lambda), y^i(\lambda), z(\lambda))$ for $i = 1 \dots N$ represent the intersection of lines L_i with the plane with height $z(\lambda)$.

Note that the set of all means $(\bar{x}(\lambda), \bar{y}(\lambda), z(\lambda))$ comprise a line. For the plane at height $z(\lambda)$ that yields the smallest spread of points $(x^i(\lambda), y^i(\lambda)$ will be the point on that line which we choose as our answer.

The two-dimensional spread of the intersection set at a particular $z(\lambda)$ is a symmetric, positive definite, 2x2 covariance matrix

$$M(\lambda) = \begin{bmatrix} var(x^i(\lambda)) & covar(x^i(\lambda), y^i(\lambda)) \\ - & var(y^i(\lambda)) \end{bmatrix}$$

It can be shown that the covariance of the interpolalated points $(x^i(\lambda), y^i(\lambda))$ can be expressed in terms of variances of and covariances between the four elementary datasets $x^i_+, x^i_-, y^i_+, y^i_-$ as follows:

$$(1) \qquad var(x^i(\lambda)) = \lambda^2\sigma^2_{x+x+} + \lambda(1-\lambda)(\sigma^2_{x+x-} + \sigma^2_{x-x+}) + (1-\lambda)^2\sigma^2_{x-x-}$$

$$(2) \qquad var(y^i(\lambda)) = \lambda^2\sigma^2_{y+y+} + \lambda(1-\lambda)(\sigma^2_{y+y-} + \sigma^2_{y-y+}) + (1-\lambda)^2\sigma^2_{y-y-}$$

$$(3) \quad covar(x^i(\lambda), y^i(\lambda)) = \lambda^2\sigma^2_{x+y+} + \lambda(1-\lambda)(\sigma^2_{x+y-} + \sigma^2_{x-y+}) + (1-\lambda)^2\sigma^2_{x-y-}$$

where

$$\sigma^2_{x+x+} = var(x^i_+),$$

TBD

FIGURE 7. MIG vs Hourglass errors

$$\sigma^2_{x+y-} = covar(x^i_+, y^i_-),$$

etc. Note in particular that, since all the σ^2 are functions only of constants $x^i_\pm, y^i_\pm$, and N, each of the 4 terms of $M(\lambda)$ is a quadratic function of λ.

If we denote the determinant of a matrix with $|\cdot|$, the area of the 1-sigma error ellipse of $M(\lambda)$ is

$$a(\lambda) = \pi\sqrt{|M(\lambda)|},$$

i.e. the square root of a quartic (4th degree) polynomial.

We seek to minimize $a(\lambda)$, which is equivalent to minimizing the quartic polynomial

$$d(\lambda) = |M(\lambda)| = var(x^i(\lambda))var(y^i(\lambda)) - covar(x^i(\lambda), y^i(\lambda))^2$$

Note that, for efficient computation, the quadratic, linear, and constant coefficients of equations (1-3) can be computed to yield

$$var(x^i(\lambda)) = a_x\lambda^2 + b_x\lambda + c_x \tag{4}$$

$$var(y^i(\lambda)) = a_y\lambda^2 + b_y\lambda + c_y \tag{5}$$

$$covar(x^i(\lambda), y^i(\lambda)) = a_{xy}\lambda^2 + b_{xy}\lambda + c_{xy} \tag{6}$$

Given coefficients computed in equations (4-6), $d(\lambda)$ can then be expressed as

$$d(\lambda) = (a_x\lambda^2 + b_x\lambda + c_x)(a_y\lambda^2 + b_y\lambda + c_y) - (a_{xy}\lambda^2 + b_{xy}\lambda + c_{xy})^2$$

$$= (a_xa_y - a^2_{xy})\lambda^4 + (\ldots)\lambda^3 + (\ldots)\lambda^2 + (\ldots)\lambda + (\ldots) \tag{7}$$

The value λ_{min} which yields the minimum value of $d(\lambda)$ will also determine the height $z(\lambda_{min})$ of the output ground point, and then λ_{min} can be used to interpolate the intersection set $(x^i(\lambda_{min}), y^i(\lambda_{min}))$, of which the mean $(\bar{x}(\lambda_{min}), \bar{y}(\lambda_{min}))$ constitutes the horizontal component of the output ground point.

3.3. **Empirical Equivalence with MIG.** For every MIG calculation that went into Figures 1–6, an Hourglass geolocation calculation was also performed. Figure **??** shows the actual errors in the X, Y, and Z directions from a MIG calculation (horizontal axis) versus an Hourglass calculation (vertical axis), for all of those calculations. (Every point in Figure 2 corresponds with $k = 100$ points in Figure **??**.) The scatter follows the unity line $y = x$ very closely, showing that Hourglassing yields very closely the same geolocation as MIG. (TBD: restricted graph for N¿10 or N¿20, showing outliers are gone?)

3.4. **Non-uniqueness.** It is desirable that this quartic polynomial $d(\lambda)$ have no local minima, but only a single, global minimum. Equivalently, the cubic derivative should have a single real root and two complex roots. Unfortunately, there can be degenerate arrangements of image rays with three real roots of $d'(\lambda$ and multiple minima for $d(\lambda)$.

Consider the bimodal situation depicted in Fig. **??**: images of the ground point are captured from satellite positions spaced equally around a horizontal circle, with orientations perfectly intersecting at a ground point at height z_+. To this bundle add a duplicate bundle, shifted both horizontally and downwards, to intersect at a lower height z_-. Clearly, the spread of the joint bundle at heights $z(\lambda = 0) = z_-$ and $z(\lambda = 1) = z_+$ are the same. And the spread at $z(\lambda = 1/2)$ is somewhat larger (note that the shape of $d(\lambda)$ is depicted sideways to the right). Thus $\lambda = 0, 1$ present two minima of $d(\lambda)$, and the hourglassing procedure in this case cannot provide a clear answer.

At least we can compute the exact form of $d(\lambda)$, and with standard techniques understand clearly whether such a degenerate situation were ever to present itself. (TBD: In our empirical testing in section **??**, we [never/seldom] encountered such a degenerate case, in NNNN hourglassing computations involving from 4 to 1000 images.)

3.5. **Error Estimation.** Review of Figures 4–6 suggests an empirical method of error estimation for Hourglassing. The predicted error curve in Figure 4 decreases very predictably as $1/\sqrt{N}$ (as demonstrated by Figure 5). So an alternative method for estimating the error of a MIG with N images would be to subsample $M << N$ images many times, compute the sample covariance C_M of the M-MIGs, and because of the $1/\sqrt{N}$ behavior (which is $1/N$ in variance space), predict the error of the N-MIG to be

$$C_N = \frac{C_M}{N/M}$$

.

This allows estimation of error apart from the output covariance of the N-MIG (or even of any of the M-MIG). There's not much point to this for MIG, since output covariance is a natural by-product of the MIG algorithm. But for Hourglassing, this provides a method of error estimation which requires no error information for the bundle, simply calculation of additional, smaller Hourglass calculations on many subamples, and computation and scaling of the sample covariance of the resulting set of geolocations.

The fundamental principle behind this error estimation technique, is that apriori error information is not needed for each image in the bundle, because the bundle *is* the distribution of error. For typical collections of only 2 or 4 images, the sample size is too small to reliably know whether the ray separation is a true representation of the amount of error in the system, or whether it may be concidentally large (or small). Thus a traditional MIG with apriori and aposteriori covariance, and reference variance as a consistency check, is most appropriate. But for large enough collections of images, the distribution of image rays is a reliable summary of the error of the process.

3.6. **Error Estimation Simulated Results.** To evaluate this empirical method of error estimation for Hourglassing, a subset of $N = 100$ images from $\mathcal{P}$ were chosen, and an Hourglass-geolocation computed for them. Subsets of $M \in \{25, 50, 75\}$

TBD

FIGURE 8. MIG vs Hourglass error estimation varx vs varx

were sampled from the N-set, $k \in \{100, 200, 400\}$ times, and an Hourglass-geolocation is computed for each M-subset. 3x3 sample covariance was computed for those k ground points, and then scaled by $1/(N/M) = M/N$ because of the $1/\sqrt{N}$ effect, and corrected also by a FPC factor of $(N-1)/(N-M)$, to yield the covariance estimate for the N-Hourglass. A MIG was also computed for the same N-subset, and its output covariance computed for reference. This experiment was repeated $R = 100$ times.

Figure 8 shows the variance of X from MIG vs Hourglass error estimation. The Hourglass error estimation has more spread than MIG.

REFERENCES

[1] Dolloff, John, and Reuben Settergren, "Worldview-1 Stereo Extraction Accuracy With and Without MIN Processing." ASPRS 2010.
[2] Law of large numbers citation, my stats book on the shelf at work
[3] Finite Population Correction reference, look up something
[4] Mikhail/Bethel/McGlone? Manual of Photogrammetry?